Modelling coating lifetime: first practical application for coating design

T. MACHADO AMORIM[*,1], C. ALLÉLY[1], J.P. CAIRE[2]
[1]ArcelorMittal Research Maizières-les-Metz, [2]ENSEEG
*Corresponding author: Voie Romaine 57283 Maizières les Metz, tiago.machado@arcelormittal.com

Abstract: The corrosion at cut edges is one of the most important degradation forms for galvanized steel sheets, the reason being the very unfavourable anode to cathode surface ratio in this region. Typically, the zinc layer is in the order of 5 µm to 20 µm thick compared to more than 700 µm for the steel substrate thickness. The major problems are the risks of red rust appearance at the exposed steel surface, and the risks of paint delamination in case of insufficient corrosion protection. The work presented here focuses on the development of a 2D FEM model simulating a steady state corrosion situation (salt spray test) at a cut edge, based on anodic delamination theory[1]. Modelled cut edge current density and delamination kinetics results are in good agreement with accelerated corrosion tests results.

Keywords: Modelling, galvanized steel, anodic delamination, cut edge corrosion.

1. Introduction

Cut edge corrosion is one of the most important corrosion problems facing continuous galvanized and coil coated steel. During the fabrication of the steel, the coatings are applied directly to the face of the sample; however, prior to use the band must be cut. At the cut edge, both the steel substrate and the zinc coating are exposed in cross-section

Cut edge corrosion appears in two forms (Fig.1):

- The formation of red rust on the cut edge. This may occur at very short times and is not a major problem if the corrosion stops.

- The delamination of the paint by blistering from the cut edge. This of course, is a major difficulty.

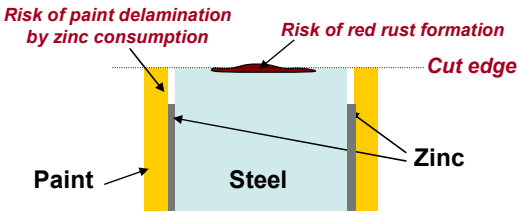

Fig. 1. Schematic cross section view of a cut edge with the 2 main corrosion risks

Galvanized steel sheets used in automotive and building industries are coated with several organic and inorganic films (Fig. 2). Such complex systems make difficult the analysis of the mechanisms involved in corrosion phenomena responsible for the paint film delamination from scratches or cut edges.

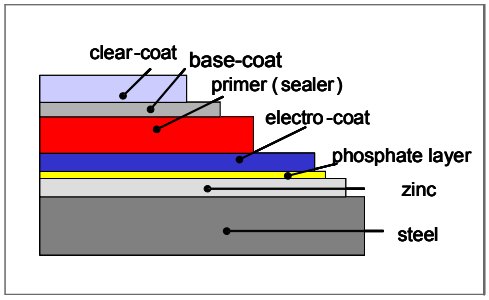

Fig. 2. Schematic representation of painted electrogalvanized steel used in automobile industry.

The standard tools employed to evaluate and improve corrosion resistance of painted systems are the accelerated corrosion tests. Nevertheless, these tests are time consuming and not always representative of the material performances in real environments.

In this context, mathematical models able to simulate systems under corrosion are a promising issue. In fact, modelling may allow the reduction of new coatings development time and help targeting films properties as function of specific problems.

2. The underpaint corrosion mechanisms on automotive samples

Numerous studies have been performed in the past years to understand the electrochemical phenomena at the origin of underpaint corrosion[1-8]. Despite of the difficulty to analyse the confined zone beneath the polymer film, the recent progress in laboratory techniques and the use of simplified systems (i.e. painted galvanized steel sheets without surface treatment) bring today new insights about how paint disbonding occurs. In fact it is now well admitted that the driving force of paint delamination is a galvanic coupling between the defect zone and the underpaint confined zone. Two different delamination mechanisms may be related to this galvanic cell existence depending upon whether the surface under the paint at the delamination front is anodic (*anodic delamination*) or cathodic (*cathodic delamination*).

To understand delamination mechanism taking place on real automobile sheets during corrosion situation, corroded scribed automobile samples have been expertised. SEM cross-section observations point out the existence of a close relation between Zn consumption and delamination phenomenon. In all the regions where paint film is detached, the Zn coat has been completely corroded (Fig. 3). The only mechanism able to explain this behaviour is **anodic delamination** which considers that delamination takes place by Zn dissolution resulting from the galvanic coupling with the steel substrate.

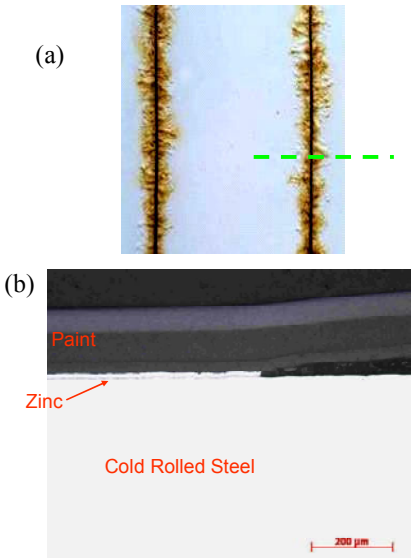

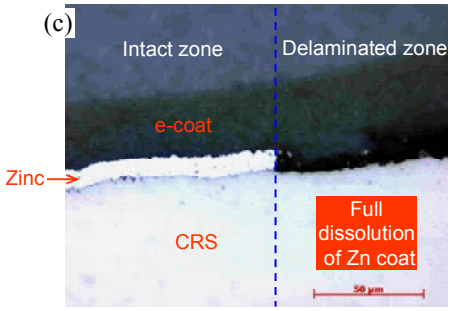

Fig. 3 (a) scribed automobile sample after accelerated corrosion test; SEM cross section of delaminated zone (x200 **(b)** and x750 **(c)**)

3. Understanding cut edge corrosion

3.1. Galvanic coupling between steel and zinc

Cut edge corrosion protection of galvanized steel sheets is guaranteed by the galvanic coupling existing between the steel substrate and the zinc film. According to Fontana et al.[10], the galvanic coupling current is created between two different metals in electric contact when they are immersed in a conductive media (electrolyte). The polarisation and the direction of the current is determined by the rest potential (E_{rest}) of each material. The one with the most important potential according to electromotive scale is the cathode. In the case of galvanized steel, Zn rest potential is equal to -1,05 V/SCE, that means 400 mV more negative than steel rest potential (E_{rest} = -0,65 (V/SCE)). In such conditions, Zn plays the role of anode and consumes itself whereas at steel surface, oxygen and water are reduced (steel is in cathodic protection).

Fig. 4 shows the polarisation curves with the main electrochemical reactions taking place at a cut edge surface in a corrosive media. This type of representation allows to determine quite easily the corrosion potential (E_{corr}) and the corrosion current (J_{corr}) resulting from the galvanic coupling between steel and zinc.

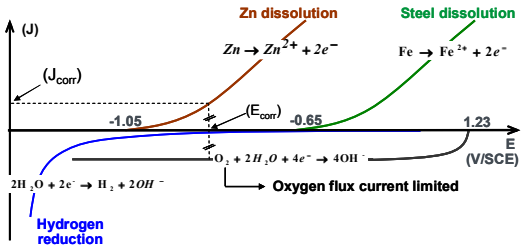

Fig. 4. Representation of main reactions taking place on a cut edge

3.2. Influence of Fe/Zn thickness ratio at a cut edge

In a more general way, corrosion at the cut edge of galvanized steel products can be considered as the worst scenario for sacrificial protection by zinc coatings, because of the very unfavourable anode to cathode surface ratio. The zinc layer is indeed in the order of 5 µm to 20 µm thick as compared to more than 700 µm for the steel substrate[11]. Fig. 5 shows the impact of Fe/Zn surface ratio on corrosion potential: for the ratio Fe/Zn=1, E_{corr} is very close to Zn rest potential, avoiding Fe corrosion. When this ratio increases, E_{corr} shifts towards Fe rest potential, reducing the cathodic protection power of the system.

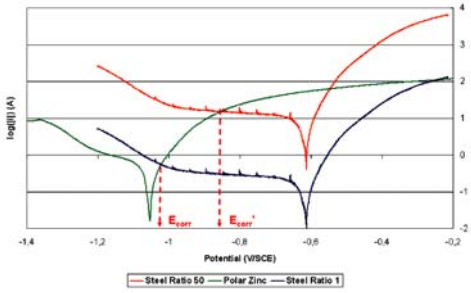

Fig. 5. Polarisation curves representing the galvanic coupling for ratio Fe/Zn=1 (blue curve) and for ratio Fe/Zn=50 (orange curve).

Despite the important Fe/Zn ratio applied to automobile products (Fe/Zn ratio close to 50 for standard auto configuration), it is well known that this configuration is satisfying to guarantee the cathodic protection of steel at cut edges.

In order to better understand the effect of Zn coating thickness on steel cathodic protection, cut edge modelling approach has its interest, being a fast and not expensive method able to bring relevant information on the maximum Fe/Zn thickness ratio able to guarantee steel cathodic protection.

4. Modelling cut edge corrosion at initial time

The developed model simulates the galvanic coupling at the cut edge without considering any change in the system geometry. The interest of this preliminary model is only to simulate the galvanic coupling at the cut edge, and then to see the effect of Fe/Zn thickness ratio on the steel cathodic protection in the first steps of corrosion.

4.1. System geometry

The mathematical model conceived in COMSOL Multiphysics is a 2D system, simulating the galvanic coupling taking place at a cut edge immersed in a 1mm thick NaCl 0,03M electrolyte. This system is in contact with atmosphere, allowing the dissolution of oxygen in the electrolyte. Three different cut edge configurations have been conceived (Table 1).

Steel thickness (µm)	Zinc thickness (per face) (µm)	Ratio Fe/Zn
800	8	50
800	2	200
800	0.5	800

Table 1. Steel and Zn thickness applied in the conception of cut edge corrosion modelling.

The first one simulates automobile configuration, with Fe/Zn thickness ratio equal to 50: steel substrate of 800 µm thick coated on both sides by a 8 µm thick Zn coating (Fig. 6).

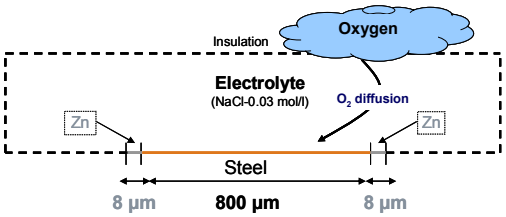

Fig. 6. Cut edge model configuration

The two other configurations have a Fe/Zn ratio of 200 and 800: constant thickness for steel substrate (800 µm), and zinc thickness of 2 and 0,5 µm respectively (both sides). The geometry from all of configuration has then been completed by a paint film of 600 µm on both sides (Fig. 7).

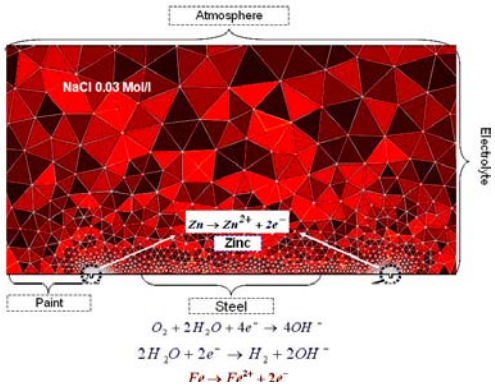

Fig. 7. COMSOL Multiphysics representation from cut edge modelling with its mesh, main reactions

4.2. Governing equations in the electrolyte

For the modelling work the application modes used in COMSOL Multiphysics were:

→ **Nernst Planck** to simulate ionic flux in the electrolyte.

→ **Diffusion** to simulate oxygen flux from atmosphere to zinc surface.

The main species present in the electrolyte are: $Na^+, Cl^-, Zn^{2+}, OH,^-$ and dissolved oxygen.

The mass balance equation controls the variation of the concentration (C_I) of the species in the medium:

$$\frac{\partial c_i}{\partial t} = -\nabla \cdot N_i + R_i$$

with R_i, the component of the chemical reactions, N_i the component corresponding to species flux. For dissolved species in an aqueous medium belonging to an electrochemical system, Ni expression is given by Nernst-Planck equation:

$$N_i = -z_i u_{mi} \nabla \phi - D_i \nabla c_i$$

where the contribution of the convection is neglected. The first term represents the contribution of migration to ionic species transport. This term is composed by the electric charge of the species (z_i), the electric potential (ϕ) and the ionic mobility (u_{mi}) which can be rewritten starting from the relation of Nernst-Einstein as being: $u_{mi} = \frac{D_i}{RT}$ (specie diffusion coefficient D_i, universal constant of gases R, and temperature of the system T). The second term represents the diffusion contribution. It is expressed by the diffusion coefficient D_i and the local species concentration gradient ∇c_i

The electroneutrality is the assumption made allowing the system to find the equilibrium between unknowns and equations:

$$\sum z_i c_i = 0$$

With z_i the electric charge of the ionic species "*i*" and c_i their concentration.

4.3. Boundary settings

The main electrochemical reactions taking place at the cut edge are zinc dissolution, oxygen & water reduction, and iron dissolution (if the coupling does not protect steel).

a) Zinc corrosion $Zn \leftrightarrow Zn^{2+} + 2e^-$

We consider here only the forward reaction, corresponding to zinc dissolution, because the backward reduction reaction is negligible. The current density for zinc dissolution is expressed by Bulter-Volmer equation:

$$j_{Zn} = j_{0,Zn} \cdot e^{\left(\frac{V - E^{\theta}_{Zn}}{\beta_{Zn}}\right)}$$

where V is the interfacial potential, β the Tafel slope, E the effective equilibrium potential, and $j_{0,Zn}$ the exchange current density.

b) Oxygen reduction: $O_2 + 2H_2O + 4e^- \rightarrow 4OH^-$

Because the kinetics of this reaction at steel surface is high and the solubility of oxygen in water is low (~ 10^{-3} M), the transport of oxygen towards the steel surface is the limiting factor of the overall corrosion kinetics. Fick's law is used to simulate this mass transport limitation and to calculate the current density of oxygen reduction at steel surface:

$$j_{lim,O_2} = nFD_{O_2} \frac{\partial c_{O_2}}{\partial z}$$

where the parameters of the equation are the number of electrons exchanged in the reaction (n), the Faraday (F) and the bulk oxygen concentration ($c_{O_2,\infty}$).

c) Water reduction: $2H_2O + 2e^- \rightarrow H_2 + 2OH^-$

The current density due to water reaction is expressed by Bulter-Volmer equation:

$$j_{H_2O} = -j_{0,H_2O} \cdot e^{\left(-\frac{V - E^{\theta}_{H_2O}}{\beta_{H_2O}}\right)}$$

d) Iron dissolution $Fe \leftrightarrow Fe^{2+} + 2e^-$

The current density due to iron corrosion is given by Bulter-Volmer equation and can be expressed as:

$$j_{Fe} = j_{0_{Fe}} \cdot e^{\left(\frac{V - E^{\theta}_{Fe}}{\beta_{Fe}}\right)}$$

e) Flux of ionic species from boundaries

Faraday's law represented by the expression: $it = n_i z_i F$ has been correlated with the notion of the species flux from the boundaries $\frac{n_i}{st} = N_i$ in order to simulate the flows of Zn^{2+} and OH^- ions from the cut edge:

$$N_{Zn^{2+}} = \frac{j_{Zn}}{2F} \quad N_{OH^-} = \frac{j_{O2}}{-F}$$

4.4. Input physical and kinetics data

Kinetics data have been obtained from polarisation curves using zinc and steel as working electrodes immersed in a 0,03M NaCl electrolyte (Table 2).

Butler Volmer	Fe $_{Oxidation}$	Zn $_{Oxidation}$	H_2O $_{reduction}$
J° (A/m²)	0.71	0.71	10^{-4}
B (V/decade)	39.0625	39.0625	19.49
E_{eq} (V/SHE)	-0.42	-0.756	-0.42

Table 2. Kinetics data for reactions on bare zinc surface

Physical data for the species diffusion coefficients have been obtained from the article of .T.Chin[12] and the ionic mobility values from the Nernst-Einstein equation (Table 3).

	Zn^{2+}	OH^-	Na^+	Cl^-	O_2
Diffusion coefficient $D*10^9$ (m^2/s)	0.712	5.24	1.33	2.03	1.90
Ionic Mobility u_m*10^{13} ($s*mol/K$)	2.86	21.04	5.31	7.84	

Table 3. Physical data for species present in the electrolyte

4.5. Modelling results

Fig. 8 shows the total current density distribution along the cut edge for the three different Fe/Zn ratios. Anodic current is located at Zn surface (positive values), and cathodic current at steel surface (negative ones).

The influence of Fe/Zn ratio is clearly visible in the cathodic zone, where the resulting current regularly decreases with Fe/Zn ratio increasing. From the simulations, it is observed that even for the extreme ratio Fe/Zn=800, the galvanic coupling is able to guarantee the protection of steel at the very beginning of corrosion situation. Nevertheless, this representation is not fully satisfying because the analysis is made on the total cathodic current, which is the sum of oxygen reduction current plus eventually iron dissolution current. That means that the negative value of total current at steel surface does not guarantee that steel is in full cathodic protection. The determination of Fe dissolution current is necessary to assess the real effect of Fe/Zn ratio on the risk of steel corrosion (Table 4).This calculation shows that the cathodic protection of steel is very efficient for Fe/Zn ratios 50 and 200 (table 4). For R = 800, steel corrodes at a rate that is 15% of pure steel corrosion kinetics; in this last condition, steel cathodic protection is not fully satisfying.

	Ratio Fe/Zn =50	Ratio Fe/Zn=200	Ratio Fe/Zn=800	Pure Steel
Steel corrosion kinetics (j_{Fe} (A/m^2))	0,0006	0,0018	0,062	0,40
Current value relative to pure steel	0,15 %	0,45 %	15,5 %	100 %

Table 4: Steel dissolution rate as function of Fe/Zn ratio at the cut edge and comparison with pure steel corrosion rate

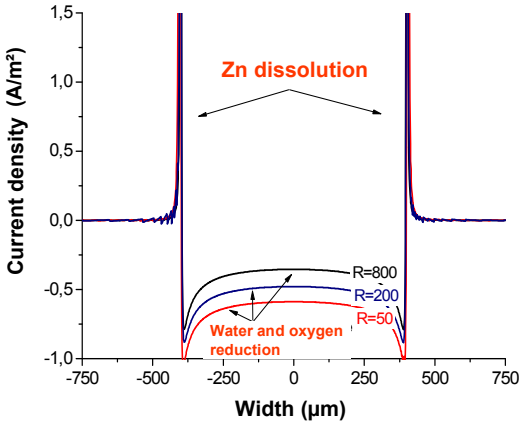

Fig. 8. Modelling total current density on cut edge for three different Fe/Zn ratio

5. Dynamic cut edge corrosion modelling / Delamination by zinc consumption

5.1. System geometry

The model described before is not sufficient to simulate the cathodic protection evolution and the paint film delamination. In fact, zinc dissolves during corrosion, inducing changes in the cut edge geometry. The consequence is a constant evolution of current distribution as far as corrosion proceeds.

To overcome this problem, a dynamic model has been conceived, with the same initial configuration as the “time zero” cut edge model (Fig. 9). Two main objectives are aimed through this dynamic model:

- Obtain the tendency concerning cathodic protection duration as function of Fe/Zn ratio.

- Determine the paint delamination rate due to zinc consumption during coupling with steel, as a function of Fe/Zn ratio at the cut edge.

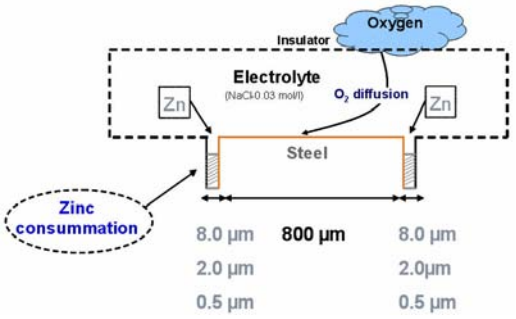

Figure 9. Configuration of dynamic cut edge corrosion model

5.2. Mathematical modelling

The basis of the dynamic cut edge model is the same as the former "time zero" model. The main differences are:

- Solver system is time dependent
- Addition of COMSOL MOBILE MESH module, allowing the cut edge's geometry evolution with Zn dissolution due to the galvanic coupling with steel. The Zn dissolution rate takes place according to Faraday's law: $it=n_i z_i F$.

5.3. Main results

The dynamic model allows the determination of delamination front as a function of corrosion time. Fig. 10 shows the systems geometry and potential in the electrolyte at initial corrosion time (time = 0) for the cut edge configuration ratio Fe/Zn=50. Fig. 11 represents the results of simulation for the same system after 11 days of corrosion time (simulation of stationary corrosion conditions similar to a salt spray test). On this type of representation, we clearly identify the front of delamination and the delamination length which is about 2 mm in the considered example.

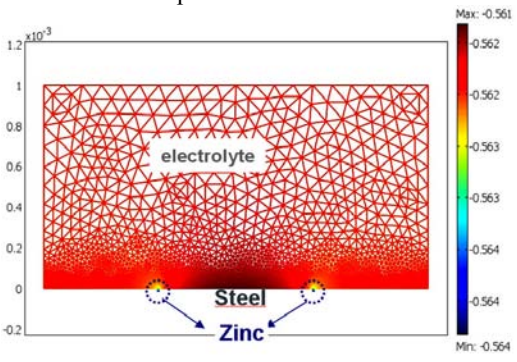

Fig. 10. Electrochemical potential at time=0 of cut edge system corresponding to ratio Fe/Zn=50

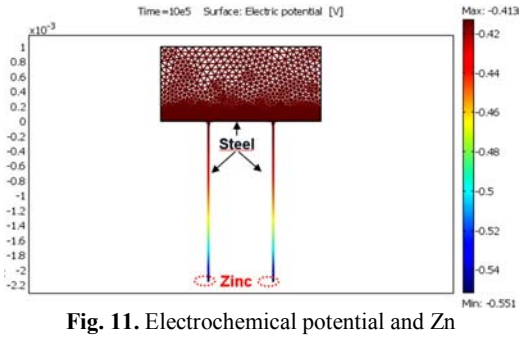

Fig. 11. Electrochemical potential and Zn consumption after time=11 days of salt spray test. Cut edge system configuration: ratio Fe/Zn=50

The model also gives the possibility to analyse the potential evolution at the steel surface as a function of zinc corrosion. By this way, it becomes possible to determine the duration of cathodic protection by calculating the time necessary to steel surface potential to achieve Fe equilibrium potential (E_{eq}=-0.42 V/SHE, table 2). This calculation has been made for each model configuration (Ratio Fe/Zn = 50; 200; 800) and the results are plotted Fig. 12.

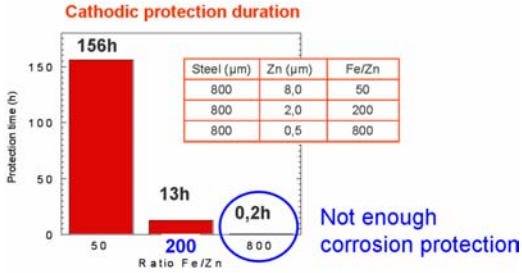

Fig. 12. Cathodic protection duration in function of ratio Fe/Zn

The obtained values do not correspond to real conditions, because of model hypothesis and simplifications, but the tendencies are quite relevant. The results confirm that ratio Fe/Zn=800 does not confer an acceptable corrosion protection to steel: the protection well exists in initial conditions, but is lost only after a few minutes when the electrolyte potential achieves Fe equilibrium one, allowing steel dissolution to occur. The other important tendency that can be simulated by the dynamic model is the influence of Zn thickness on delamination rate. This phenomenon has been observed in accelerated corrosion tests results (Fig. 13) and on vehicle tests (Fig. 14), with a delamination rate that increases when the coating thickness decreases for a same steel substrate.

Nevertheless this observation has never been associated with any delamination mechanisms.
The simulations made with the model clearly point out the important effect of zinc coating thickness or Fe/Zn ratio on the delamination rate (Fig. 15). These results are in good agreement with experimental data, and point out anodic delamination as being the most relevant mechanism for underpaint corrosion of automobile systems.

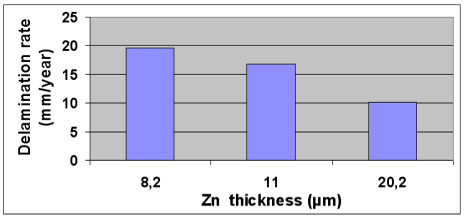

Fig. 13. Cosmetic corrosion delamination results for 10 VDA cycles

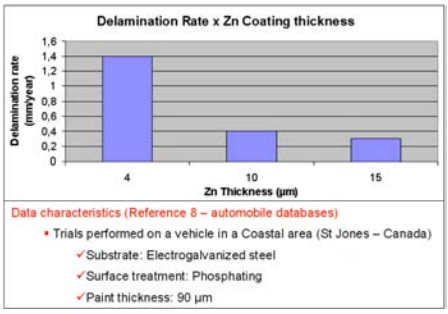

Fig. 14. On-vehicle cosmetic corrosion delamination results (KIMAB Database)

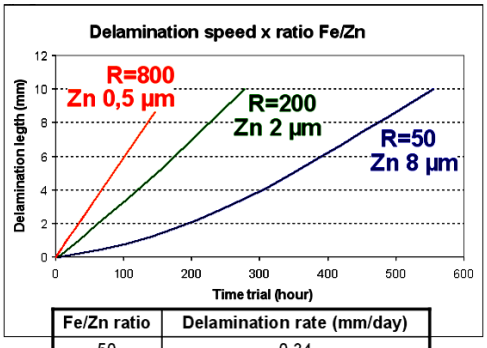

Fe/Zn ratio	Delamination rate (mm/day)
50	0,34
200	0,72
800	1,49

Fig. 15. Delamination rate x Zn thickness (anodic delamination mechanism)

6. Conclusions

The model simulating the cut edge corrosion has been developed in COMSOL Multiphysics environment. It is a 2D model that uses Nernst Planck and Mobile Mesh to calculate a cathodic protection evolution with Zn consumption and delamination rate for different Fe/Zn systems. ARSA model results are in good agreement with literature and experimental trials for simplified system submitted to steady state corrosion conditions.
The model clearly explains the influence of the surface ratio between steel and zinc at a cut edge on the delamination phenomena for real automobile systems. Anodic delamination appears as being the most relevant mechanism for such real painted systems.

References

1. C. R. Shastry, H. E. Townsend, *Corrosion Science*, 45 103 – 119 (1989).
2. K. N. Allahar, K. Ogle, Mark Orazem, *Critical Factors in Localized Corrosion IV - A Symposium in Honor of the 65th Birthday of Hans Bohni, Ed. by S. Virtanen, P. Schmuki, G. S. Frenkel*, p474.
3. K. N. Allahar, Mathematical modelling of disbonded coating and cathodic delamination systems*, Dissertation Florida University* (2003).
4. A. Leng, H. Streckel, and M. Stratmann, *Corrosion Science*, 41, 547–578 (1999).
5. A. Leng, H. Streckel, and M. Stratmann, *Corrosion Science*, 41, 579–597 (1999).
6. W. Furbeth and M. Stratmann, *Corrosion Science*, 43, 207–227 (2001).
7. W. Furbeth and M. Stratmann, *Corrosion Science*, 43, 229–241 (2001).
8. W. Furbeth and M. Stratmann, *Corrosion Science*, 43, 243–254 (2001).
8. D.D. Davidson and W.A. Schumarcher, *Conf. SAE, Dearborn, MI*., Paper No. 1991, Paper No. 396, (1991)
9. D. Massinon, D. Dauchelle, J. C. Charbonnier *Mater. Sci. Forum*, 461, 44-45 (1980)
10 Fontana, M. G., et al., *Corrosion engineering*, 2nd ed., McGraw-Hill, New York, (1978)
11. K. Ogle, V.Baudu, L.Garrigues, *Journal of the Electroch. Soc.*, 147, 3654-3660 (2000).
12. D.T. Chin and G.M; Sabde, *Corrosion*, 56, No 8

Acknowledgements

We would like to thank the European Union's 6th framework programme for financial support (project contract number: STRP 01376).